Ab initio elastic stiffness of nano-laminate ($M_xM'_{2-x}$)AlC (M and M' = Ti, V and Cr) solid solution

2004 J. Phys.: Condens. Matter 16 2819

(http://iopscience.iop.org/0953-8984/16/16/006)

INSTITUTE OF PHYSICS PUBLISHING JOURNAL OF PHYSICS: CONDENSED MATTER

J. Phys.: Condens. Matter **16** (2004) 2819–2827 PII: S0953-8984(04)76212-8

Ab initio elastic stiffness of nano-laminate $(M_xM'_{2-x})AlC$ (M and M′ = Ti, V and Cr) solid solution

J Y Wang[1,2] **and Y C Zhou**[1]

[1] Shenyang National Laboratory for Materials Science, Institute of Metal Research, Chinese Academy of Sciences, Shenyang 110016, People's Republic of China
[2] International Centre for Materials Physics, Institute of Metal Research, Chinese Academy of Sciences, Shenyang 110016, People's Republic of China

Received 6 February 2004
Published 8 April 2004
Online at stacks.iop.org/JPhysCM/16/2819
DOI: 10.1088/0953-8984/16/16/006

Abstract

We have investigated the elastic stiffness and electronic band structure of nano-laminate $(M_xM'_{2-x})AlC$ solid solutions, where M and M′ = Ti, V and Cr, by means of the *ab initio* pseudopotential total energy method. The second-order elastic constants, bulk moduli and anisotropic Young's moduli are computed for the solid solutions, in which x is changed from 0 to 2 in steps of 0.5. The bulk moduli of $(M_xM'_{2-x})AlC$ is found to be approximately the average of the two end M_2AlC and M'_2AlC phases as the substitution content x, as well as the valence electron concentration (VEC), varies in the compounds. On the other hand, the shear modulus c_{44}, which by itself represents a pure shear shape change and has a direct relationship with hardness, saturates to a maximum as VEC is in the range 8.4–8.6. It implies that solid solution hardening may be operative for alloys having VEC values in this range. Furthermore, trends in the elastic stiffness are interpreted in terms of the electronic band structure. We show that monotonically incrementing the bulk moduli is attributed to the occupying states involving transition-metal d–Al p covalent bonding and metal-to-metal dd bonding. The maximum in c_{44}, on the other hand, originates from completely filling the shear resistive transition-metal d–Al p bonding states. Most importantly, we predict a method to optimize the desired elastic stiffness by properly tuning the valence electron concentration of $(M_xM'_{2-x})AlC$ ceramics.

(Some figures in this article are in colour only in the electronic version)

1. Introduction

Among the so-called M_2AX phases (where M is an early transition metal atom, A is an A-group element and X is carbon and/or nitrogen), Ti_2AlC has been widely studied due to the fact that it has overall advantages [1]. For example, it displays a combination of such properties as high melting point, low density, high bulk modulus, good thermal and electrical conductivity, excellent thermal shock resistance and high temperature oxidation resistance, damage tolerance and microscale ductility at room temperature, etc. Ti_2AlC crystallizes in a space group of $P6_3/mmc$ symmetry and its crystal structure can be regarded as the nanoscale sheet of edge-shared transition-metal carbide octahedra being weakly bonded with the interleaved planar close-packed Al atomic layers. According to this unique nano-laminate crystal structure, Ti_2AlC exhibits properties of both ceramics and metals and looks to be a promising candidate for high temperature structural applications.

Great efforts have been made to optimize the desired mechanical properties over the last few years for T_2AlC. According to earlier investigations, possible solutions are addressed in alloying and/or solid solution treatment. To achieve this goal, one can substitute elements on the C site with N or O. Following this idea, Barsoum *et al* [2] succeeded in strengthening Ti_2AlC by synthesizing a $Ti_2AlC_{0.5}N_{0.5}$ solid solution. Another way is to substitute Ti atoms by other transition-metal atoms, such as V, Nb and Cr. The excellent miscibility of the solid solution series on M sites in M_2AlC (M = Ti, V, Nb and Cr) systems has been confirmed both in experiments by Nowotny and coworkers [3], and in theoretical calculations by Sun *et al* [4]. Very recently, Salama *et al* synthesized $(Ti, Nb)_2AlC$ and investigated its mechanical properties [5]. Unfortunately, no solid solution hardening effect was operative in such a Ti–Nb–Al–C system. Until now, only the theoretical bulk moduli of $(M_xM'_{2-x})AlC$ compounds, where M and M′ are Ti, V and Cr, have been presented [4]. Regardless of these achievements, it is still not easy to design new complex nano-laminate ternary alloys with predictable mechanical properties. Generalized results should be presented and examined in predicting the mechanical properties of complex nonstoichiometric M–Al–C compounds.

Using the correlation between elastic stiffness and hardness, many theoretical predictions on hard materials have been successfully made during the last few decades. Recently, Jhi *et al* [6] found that the magnitude of the shear modulus c_{44}, rather than the bulk modulus B and shear modulus G, was a better hardness predictor for transition-metal carbonitrides TiC_xN_{1-x}. They showed that the hardness and shear moduli c_{44} reached a maximum simultaneously when the valence electron concentration is about 8.4 in TiC_xN_{1-x}, while the bulk and shear moduli do not show the same trend. If the rule for transition-metal carbonitrides is true for the presently studied compounds, information about the bulk moduli is not sufficient for predicting the macro-mechanical properties of $(M_xM'_{2-x})AlC$, especially its hardness. In this paper, we computed the second-order elastic constants, bulk modulus and anisotropic Young's modulus of $(M_xM'_{2-x})AlC$ (M and M′ = Ti, V and Cr), and the trends in bulk modulus and shear modulus c_{44} varying with VEC are presented. Furthermore, the results are well interpreted by electronic band structure analysis. The aim of this work is to provide a predictive starting point for an investigation of complex nonstoichiometric $(M_xM'_{2-x})AlC$ compounds.

2. Computational details

A supercell with an isotropic substitution configuration should be examined to minimize the difference between theoretical modelling and random substitution in solid solutions. To achieve this, a large cell size is needed, e.g. a $2 \times 2 \times 1$ supercell with 32 atoms. Unfortunately, estimating elastic constants from first-principles calculations is still hard work because it

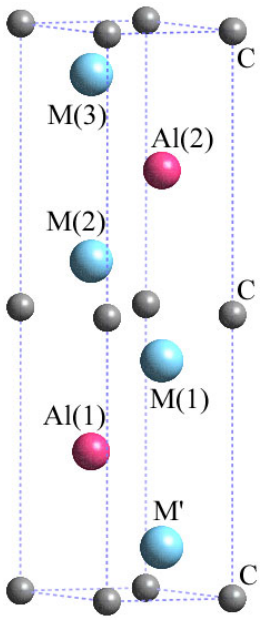

Figure 1. Crystal structure of $M_xM'_{2-x}AlC$ solid solution.

requires accurate methods for evaluating the total energy or stress accompanying the strain. Therefore, we constructed the solid solution in the unit cell because of the current limits of our available computers. Similar lattice configurations were used in modelling Ti_3SiC_2-base solid solutions [7] and $(M_xM'_{2-x})AlC$ compounds [4]. Figure 1 illustrates the crystal structure of $(M_xM'_{2-x})AlC$ solid solution, where M and M′ are Ti, V and Cr, and x changes from 0 to 2 in steps of 0.5. For $x = 0.5$ and 1.5, M and M′ sites are occupied by different types of transition-metal element. For $x = 1.0$, we set M(2) and M′ sites as being occupied by the same type of atom, as well as M(1) and M(3) sites being the same. Our computational results showed that this configuration yielded the lowest total energy compared to other possible configurations. In the present work, the VEC is tuned by changing the value of the substitution content x.

The present computation was based on density functional theory and the plane-wave pseudopotential total energy method was utilized [8]. Interactions of electrons with ion cores were represented by the Vanderbilt-type ultrasoft pseudopotential for transition metal M, M′, Al and C atoms [9]. The electronic exchange–correlation energy was treated under the generalized gradient approximation [10]. The plane-wave basis set cut-off was set as 450 eV for all cases. The special point sampling integration over the Brillouin zone was employed by using the Monkhorst–Pack method with a $10 \times 10 \times 2$ special k-point mesh [11]. These parameters were sufficient to lead to well converged total energy and geometrical configurations. Increasing the plane-wave cut-off energy to 700 eV and the k-point mesh to $14 \times 14 \times 2$ changed the total energy by less than 0.005 eV/atom and the lattice constants by less than 0.02%.

Lattice parameters, including lattice constants and internal atomic coordinates, were modified independently to minimize the total energy, interatomic forces and stresses of the unit cell. The Brodyden–Fletcher–Goldfarb–Shanno (BFGS) minimization scheme [12] was used in geometry optimization. The tolerances for geometry optimization were set as the difference in total energy being within 5×10^{-6} eV/atom, the maximum ionic Hellmann–Feynman force to being within 0.01 eV Å^{-1}, the maximum ionic displacement to being within 5×10^{-4} Å and the maximum stress to being within 0.02 GPa.

The elastic coefficients were determined from first-principles calculation by applying a set of given homogeneous deformations with a finite value and calculating the resulting stress with respect to optimizing the internal atomic freedoms, as implemented by Milman *et al* [13]. The criteria for convergences of optimization on atomic internal freedoms was selected as the difference in total energy being within 1×10^{-6} eV/atom, the ionic Hellmann–Feynman forces being within 0.002 eV Å^{-1} and the maximum ionic displacement being within 1×10^{-4} Å. For stoichiometric M_2AlC phases with $P6_3/mmc$ symmetry, two strain patterns, one with non-zero ε_{11} and ε_{23} components and another with a non-zero ε_{33}, brought out stresses related to all five independent elastic coefficients. Whereas, for a $(M_xM'_{2-x})AlC$ solid solution with $P3m1$ symmetry, two strain patterns, one with non-zero ε_{33} and ε_{23} components and another with a non-zero ε_{11}, brought out stresses related to all seven independent elastic coefficients. Three positive and three negative amplitudes were applied for each strain component, with the maximum strain value of 0.5% in all computations. The elastic stiffness was determined from a linear fit of the calculated stress as a function of strain. The compliance matrix, S, was calculated as the inverse of the stiffness matrix, $S = C^{-1}$. Other elastic mechanical parameters, such as bulk modulus and Young's modulus, were calculated from the compliance matrix components.

3. Results and discussions

3.1. Dependence of elastic stiffness on VEC

Table 1 includes our computed second-order elastic constants for $(M_xM'_{2-x})AlC$, where M and M′ = Ti, V and Cr, respectively. The moduli c_{14} and c_{15} are less than 2 GPa for all the solid solutions. Therefore they are not presented in table 1. Bulk moduli and anisotropic Young's moduli are calculated from the elastic compliance matrix and are also listed in table 1. It is noted that the solid solutions are essentially elastically anisotropic because the Young's moduli are evidently different along directions on the basal plane and six-fold symmetry axis. Our computed bulk moduli are about 30–40 GPa smaller than those presented by Sun *et al* [4]. Although the discrepancy is still not fully understood, we attribute it to the computational method employed. Up to now, no direct experimental bulk modulus is available to be compared with our theoretical results. Therefore, we choose Ti_3AlC_2 as a reference compound, which has close relationships with M_2AlC not only in crystal structure but also in macro-properties. The computed results of Ti_3AlC_2 yield 160 GPa for the bulk modulus and 131 GPa for the shear modulus, while the experimental values are 165 and 124 GPa [14], respectively. Good agreement between computational and experimental values is achieved, which ensures the reliability of the computed data for the $(M_xM'_{2-x})AlC$ phases.

The bulk moduli of the $(M_xM'_{2-x})AlC$ phases as a function of VEC are plotted in figure 2(a), where the broken lines represent the average value of the two end M_2AlC and M'_2AlC phases for various substitution contents. We note that the bulk modulus of $(M_xM'_{2-x})AlC$ is close in magnitude to the average value for the substitution content x (as well as the VEC) changes: $B_{M_xM'_{2-x}AlC}(x) \cong xB_{M_2AlC} + (2-x)B_{M'_2AlC}$. The deviation from the average data is within 4 GPa for all compounds considered in the present work, which indicates that the bulk moduli of $(M_xM'_{2-x})AlC$ systems are well related to a generalized parameter x (as well as the VEC). It further indicates that the bulk modulus is predictable when tuning the chemical content in the solid solutions. The bulk moduli of solid solutions increase monotonically as VEC increases, and improve more effectively in going from Ti_2AlC to V_2AlC than from V_2AlC to Cr_2AlC. The bulk modulus is increased by 38 GPa when V atoms completely replace the Ti atoms. As one proceeds from V_2AlC to Cr_2AlC, the bulk modulus increases by only 18 GPa.

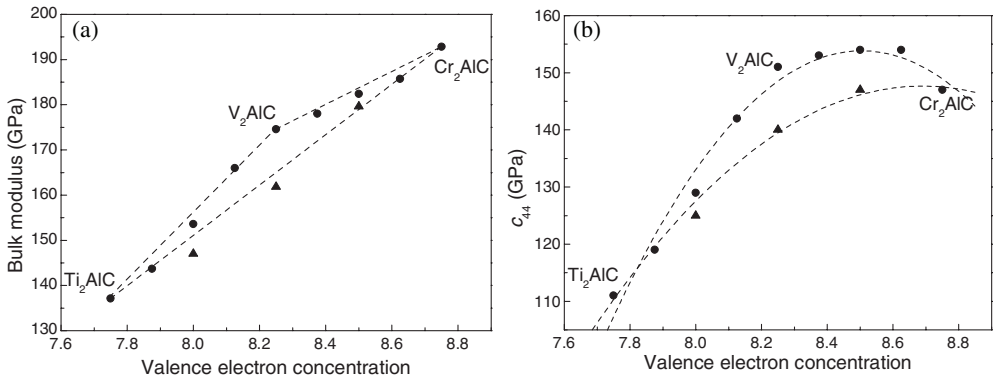

Figure 2. Theoretical (a) bulk moduli and (b) shear moduli c_{44} of $M_xM'_{2-x}AlC$ as a function of valence electron concentration. Full circles represent the results of $Ti_xV_{2-x}AlC$ and $V_xCr_{2-x}AlC$, and triangles represent the data of $Ti_xCr_{2-x}AlC$.

Table 1. Calculated second-order elastic constants c_{ij} (in GPa), bulk modulus B_0 (in GPa) and Young's modulus E (in GPa) of $M_xM'_{2-x}AlC$ (M, M′ = Ti, V and Cr).

	c_{11}	c_{12}	c_{13}	c_{33}	c_{44}	B_0	E
Ti_2AlC	308	55	60	270	111	137	$E_x = 290$ $E_z = 250$
$Ti_{1.5}V_{0.5}AlC$	291	53	83	275	119	144	$E_x = 263$ $E_z = 235$
TiVAlC	300	78	89	272	129	154	$E_x = 262$ $E_z = 230$
$Ti_{0.5}V_{1.5}AlC$	335	75	92	308	142	166	$E_x = 299$ $E_z = 267$
V_2AlC	346	71	106	314	151	175	$E_x = 306$ $E_z = 261$
$V_{1.5}Cr_{0.5}AlC$	359	72	105	319	154	178	$E_x = 303$ $E_z = 260$
VCrAlC	358	75	111	331	153	183	$E_x = 315$ $E_z = 273$
$V_{0.5}Cr_{1.5}AlC$	363	73	114	344	154	186	$E_x = 321$ $E_z = 284$
Cr_2AlC	384	79	107	382	147	193	$E_x = 347$ $E_z = 332$
$Cr_{1.5}Ti_{0.5}AlC$	349	71	93	316	147	170	$E_x = 316$ $E_z = 275$
CrTiAlC	325	70	91	302	139	162	$E_x = 292$ $E_z = 261$
$Cr_{0.5}Ti_{1.5}AlC$	311	58	77	283	124	147	$E_x = 285$ $E_z = 251$

When predicting the hardness, one should go beyond the bulk modulus and consider the shear modulus. According to the Voigt approximation, the shear modulus G, on the one hand, is not a good candidate for a hardness predictor because it is also an *average* of single-crystal

elastic constants [15]:

$$G_{\mathrm{V}} = \tfrac{1}{15}(2c_{11} + c_{33} - c_{12} - 2c_{13}) + \tfrac{1}{5}(2c_{44} + c_{66}) \quad (1)$$

for a unit cell with hexagonal symmetry. On the other hand, only the c_{44} (rather than the c_{66}, the difference between c_{11} and c_{12}), among the various shear stiffnesses, by itself represents a shape change without volume change and provides direct information about the hardness involved in indentation [6]. Therefore, we examine the correlation between c_{44} and VEC for $(M_xM'_{2-x})AlC$ compounds.

Figure 2(b) illustrates the computed c_{44} at various VEC for $(M_xM'_{2-x})AlC$ solid solutions. The upper broken curve is the polynomial fit to the theoretical c_{44} of $Ti_xV_{2-x}AlC$ and $V_xCr_{2-x}AlC$ solid solutions, and the lower curve is that for $Ti_xCr_{2-x}AlC$. One should note in figures 2(a) and (b) that the elastic moduli of $Ti_xCr_{2-x}AlC$ are smaller than those of $Ti_xV_{2-x}AlC$ and $V_xCr_{2-x}AlC$ when the VEC yields the same value. This can be explained by the larger atomic size and valence electron differences between Cr and Ti, which lead to less phase stability of $Ti_xCr_{2-x}AlC$ [4]. The most interesting feature is that the shear modulus c_{44} saturates to a maximum value for VEC in the range 8.4–8.6. A similar trend was observed for transition-metal carbonitrides, in which the c_{44} and micro-hardness simultaneously reach a maximum at the VEC value of ∼8.4 [6]. If the rules for transition-metal carbonitrides are applicable to the presently studied compounds, this class of ternary carbides would exhibit maximal hardness for VEC in the appropriate range. In other words, solid solution hardening might be operative in $V_xCr_{2-x}AlC$ alloys in a certain VEC range.

3.2. Electronic band structure

To understand the trends in elastic moduli common to all these materials on a fundamental level, the characteristics of the electronic band structure of $(M_xM'_{2-x})AlC$ are examined. We intend to interpret the trends in elastic stiffness by illustrating the occupation of additional valence electrons in certain electronic states. It is found that the features of electronic band dispersion curves and total DOS (e.g. the peak structures and relative heights of the peaks in DOS) are rather similar, which shows that the electronic structure is well described by the rigid-band model for $(M_xM'_{2-x})AlC$. Therefore, taking $V_{0.5}Cr_{1.5}AlC$ as an example, the electronic structure is representatively discussed in the present paper.

Characteristics of atomic bonding can be clearly illustrated by the projected density of states (PDOS). We perform the projection of the plane-wave electronic states onto a localized linear combination of atomic orbital basis sets. Then the total electronic DOS is decomposed according to site and angular momentum. The PDOS of $V_{0.5}Cr_{1.5}AlC$ is illustrated in figure 3. The states, which are approximately located between −7.5 and −3.5 eV below the Fermi level, originate from the hybridization of transition-metal 3d–C 2p orbitals. Detailed electronic band structure analysis demonstrates that the peaks located at about −4.5 and −4.0 eV below E_{F} are due to the hybridization of $d(t_{2g})$–(p_x, p_y) and $d(t_{2g} + e_{2g})$–p_z bonding states between transition-metal and carbon atoms, respectively. The states located at adjacent higher energy levels, extending between −3.7 and −1.0 eV, are dominated by $d(e_g)$–p covalent bonding orbitals between transition-metal and Al atoms. The largest contribution to states near Fermi level comes from metal-to-metal dd interactions.

The bonding states derived from M(M′)–C dp interactions are located far below the Fermi level and are disturbed slightly as VEC varies. Therefore, theoretical trends in elastic stiffness are decided by characteristics of bonding states near the Fermi level. Attentions are concentrated to occupation of M(M′)–Al dp bonding and metal-to-metal dd bonding. The occupation of pd bonding states can be illustrated by examining the energy range of M(M′)–Al dp bonding states in solid solutions. For the case of V_2AlC, the energy level of V–Al dp

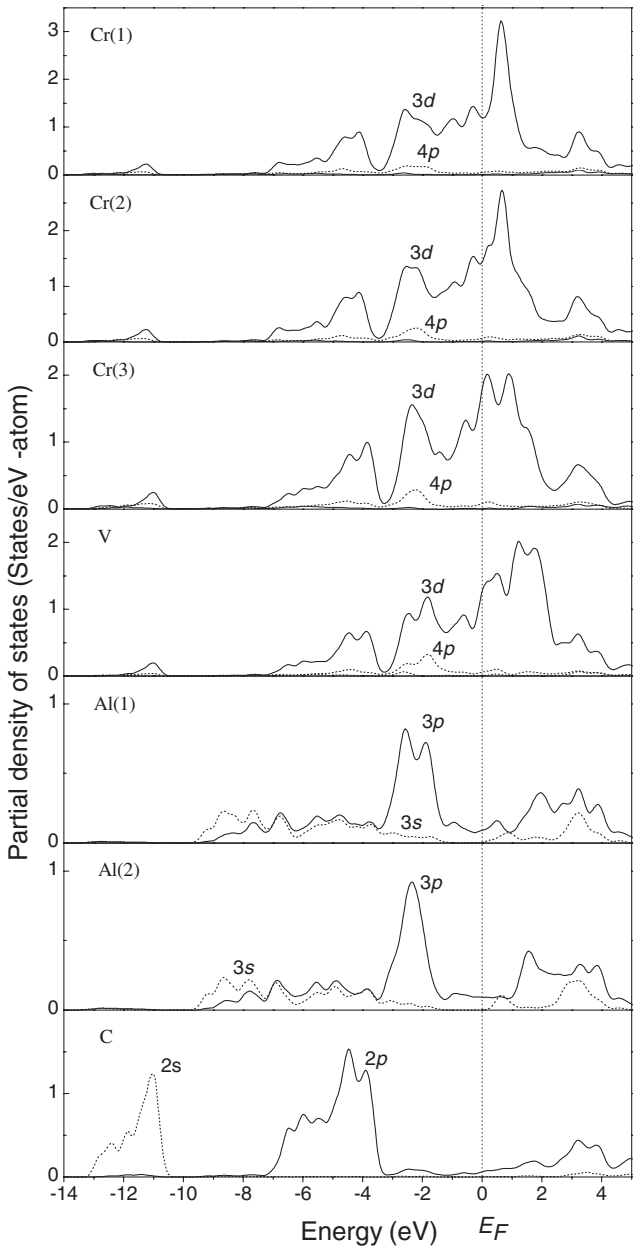

Figure 3. Site and angular momentum projection of the electronic density of states of $V_{0.5}Cr_{1.5}AlC$.

bonding states spreads from −3.388 to 0.258 eV, which indicates that these states are partially occupied, whereas the energy level of the V(Cr)–Al dp bonding states shifts downward and extends from −3.732 to −0.956 eV in $V_{0.5}Cr_{1.5}AlC$, which shows that the corresponding states are completely filled. We also examine the corresponding energy level in $V_{1.5}Cr_{0.5}AlC$ and the value extends from −3.435 to −0.618 eV. Therefore, the M(M′)–Al dp bonding starts to saturate as VEC is located between those of V_2AlC and $V_{1.5}Cr_{0.5}AlC$.

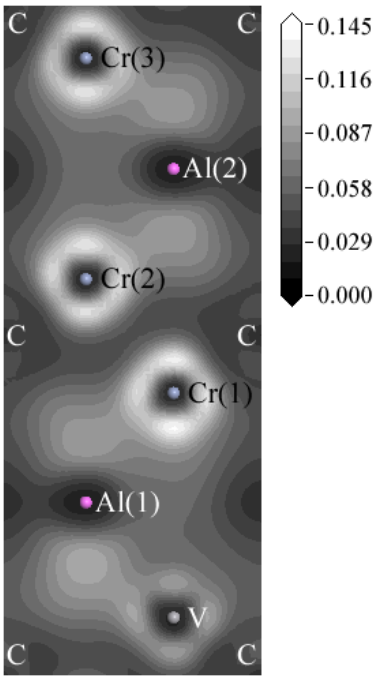

Figure 4. Valence electron density of M(M′)–Al pd bonding in $V_{0.5}Cr_{1.5}AlC$. The plot is in the $(11\bar{2}0)$ plane and the unit is electrons/Å^3.

According to the discussions, trends in moduli as VEC is varying can be exactly understood in terms of electronic structure. Figure 2(a) shows that the moduli increase more significantly in going from Ti_2AlC to V_2AlC than from V_2AlC to Cr_2AlC. The reason is attributed to different occupation of valence electrons in various solid solutions. The valence electrons progressively fill pd bonding states in the $Ti_xV_{2-x}AlC$ system and lead to effectively improved bulk moduli, whereas, in the $V_xCr_{2-x}AlC$ solid solutions, the pd bonding states saturate, starting from $V_{1.5}Cr_{0.5}AlC$. In turn, nearly all the extra valence electrons fill the d orbitals provided by transition-metal atoms. Grossman *et al* [16] computed the bulk modulus of some selected first-row transition-metal solids and found that the bulk modulus of pure elements increased as the number of valence electrons increased. Thereby, enhancement of the dd metallic interactions is also beneficial to enhance the bulk moduli of the $(M_xM'_{2-x})AlC$ phases.

On the other hand, shear stiffness c_{44} is effectively increased only by strengthening the M(M′)–Al pd covalent bonding. The maximum in c_{44} originates from the complete filling of the shear resistive dp-derived bonding states between M(M′) and Al atoms. Excessive occupation of the dd bonding gives rise to a negative contribution to the elastic shear resistance, such as the reduced c_{44} of Cr_2AlC. Similar phenomena have been reported for transition-metal carbonitrides [6].

In addition, we decompose the total charge density into contributions from M(M′)–Al pd bonding, and illustrate the result for the $(11\bar{2}0)$ plane of $V_{0.5}Cr_{1.5}AlC$ in figure 4. The unit of charge density is electrons Å^{-3} in the figure. We note that the electron densities centred on neighbouring Cr and Al atoms, and V and Al atoms, are nearly the same. Therefore, similar bonding strengths of M(M′)–Al pd covalent interactions are well established in $(M_xM'_{2-x})AlC$, which leads to predictable trends in bulk and shear stiffness.

4. Conclusions

We have predicted the theoretical elastic stiffness of nano-laminate $(M_xM'_{2-x})AlC$ solid solutions, where M and M′ are Ti, V and Cr, by means of the *ab initio* pseudopotential total energy method. Trends in bulk modulus and shear modulus c_{44} are presented for the solid solutions. The bulk modulus of $(M_xM'_{2-x})AlC$ is approximately the average of the two end M_2AlC and M'_2AlC phases as the substitution content, as well as the VEC, changes. The shear modulus c_{44}, which has a direct relationship with hardness, saturates to a maximum as VEC is in the range 8.4–8.6. Our results indicate that the elastic stiffness is predictable when tuning the chemical components in M_2AlC phases. We show that an increment of the bulk modulus contributes to additional valence electrons occupying states involving M(M′)d–Al p covalent bonding and metal-to-metal dd bonding. The maximum in c_{44}, on the other hand, originates from completely filling the shear resistive M(M′)d–Al p bonding states. In addition, a predictive method is presented to optimize the desired elastic stiffness by properly tuning the VEC of $(M_xM'_{2-x})AlC$ ceramics.

Acknowledgments

This work was supported by the National Outstanding Young Scientist Foundation by grant no 59925208 to YCZ, the Natural Sciences Foundation of China under grant nos 50232040 and 50302011, the '863' project, and the High-Tech Bureau of the Chinese Academy of Sciences.

References

[1] Wang X H and Zhou Y C 2003 *Corros. Sci.* **45** 891
[2] Barsoum M W, Ali M and El-Raghy T 2000 *Metall. Mater. Trans.* **31A** 1857
[3] Schuster J C, Nowotny H and Vaccaro C 1980 *J. Solid State Chem.* **32** 213
[4] Sun Z M, Ahuja R and Schneider J M 2003 *Phys. Rev.* B **68** 224112
[5] Salama I, El-Raghy T and Barsoum M W 2002 *J. Alloys Compounds* **347** 271
[6] Jhi S H, Ihm J, Louie S G and Cohen M L 1999 *Nature* **399** 132
[7] Medvedeva N I, Novikov D L, Ivanovsky A L, Kuznetsov M V and Freeman A J 1998 *Phys. Rev.* B **58** 16042
[8] Segall M D, Lindan P L D, Probert M J, Pickard C J, Hasnip P J, Clark S J and Payne M C 2002 *J. Phys.: Condens. Matter* **14** 2717
[9] Vanderbilt D 1990 *Phys. Rev.* B **41** 7892
[10] Perdew J P, Chevary J A, Vosko S H, Jackson K A, Pederson M R, Singh D J and Fiolhais C 1992 *Phys. Rev.* B **46** 6671
[11] Monkhorst H J and Pack J D 1977 *Phys. Rev.* B **16** 1748
[12] Fischer T H and Almlof J 1992 *J. Phys. Chem.* **96** 9768
[13] Milman V and Warren M C 2001 *J. Phys.: Condens. Matter* **13** 241
[14] Barsoum M W 2000 *Prog. Solid State Chem.* **28** 201
[15] Ravindran P, Fast L, Korzhavyi P A, Johansson B, Wills J and Eriksson O 1998 *J. Appl. Phys.* **84** 4891
[16] Grossman J C, Mizel A, Côté M, Cohen M L and Louie S G 1999 *Phys. Rev.* B **60** 6343